

Formation. Their workmanship indicates pre-existence of the culture as well, and the lower limit of this culture is yet to be established.

The artefacts recovered from the excavations have typological affinities with those from the Olduvai Gorge in Africa. It is possible that tool-making hominids of Pliocene-Pleistocene were contemporary in the two continents and have the same antiquity.

The Early Palaeolithic culture of the Siwalik region, in view of its precise antiquity and stratigraphic position, is designated here as the "Siwalik Stone Age".

The fruitful discussions in the field with Dr S. N. Rajaguru and Dr G. L. Badam are gratefully acknowledged.

19 February 1988; Revised 1 August 1988

1. Lal, B. B., *Ancient India*, 1956, 12, 58.
2. Joshi, R. V., Rajaguru, S. N., Badam, G. L. and Khanna, P. C., *J. Geol. Soc. India*, 1978, 19, 83.
3. Rajaguru, S. N., *Proc. Neogene/Quaternary Boundary Field Conference, India*, 1981, p. 127.
4. Verma, B. C., *J. Geol. Soc. India*, 1975, 16, 518.
5. Sharma, J. C., *Curr. Anthropol.*, 1977, 18, 94.
6. Verma, B. C. and Srivastava, J. P., *Man Environ.*, 1984, 8, 13.
7. Anon, *Geol. Surv. India. News Northern Region*, 1985, 5, 4.
8. Ranga Rao, A., Khan, K. N., Venkatachala, B. S. and Sastri, V. V., *Proc. Neogene/Quaternary Boundary Field Conference, India*, 1981, p. 131.
9. Yokoyama, T., Verma, B. C., Matsuda, T., Gupta, S. S. and Tewari, A. P., *Indian Min.*, 1988, (in press).

GRADE DISTRIBUTIONS IN MANGANESE NODULES OF CENTRAL INDIAN OCEAN BASIN

M. SUDHAKAR

National Institute of Oceanography, Dona Paula,
Goa 403 004, India.

ECONOMIC potential of deep-sea manganese nodules has drawn considerable attention from various organizations investigating the seabed mineral re-

sources. The factors which limit deep-sea nodule mining are the economic grade (%Co + %Ni + %Cu) and abundance (kg/m²) of nodules on seafloor. Limited data are available on nodules from the Central Indian Ocean Basin (CIOB), for resource evaluation of these deposits.

Data concerning to geological setting, physical characteristics and bulk chemical composition of the

Table 1 Transition frequencies computed for eight directions shown in matrix tables

I				II			
169	20	1	0	169	21	0	0
21	161	34	0	20	161	39	0
0	39	258	53	1	34	258	63
0	0	63	415	0	0	53	415
III				IV			
163	27	0	0	163	11	0	0
11	160	49	0	27	160	16	0
0	16	268	75	0	49	268	39
0	0	39	420	0	0	75	420
V				VI			
164	22	0	0	158	29	3	0
35	203	42	0	16	143	57	4
3	78	275	56	0	28	232	93
0	4	103	430	0	0	53	382
VII				VIII			
153	33	1	0	154	20	0	0
18	110	43	0	35	140	28	0
0	15	146	60	1	56	227	56
0	0	40	579	0	0	93	378

nodules sampled from CIOB were stored in the Computer Data Bank of this Institute. Bulk chemical composition of nodules, in which grade is expressed as %Co + %Ni + %Cu was used as input for Markov modelling studies presented here.

A grid of square cells where each grid point represents a discrete 'state' of the grade (figure 1), is divided into 4 states as paramarginal (>2.47%), submarginal A (2.47 to 2%), submarginal B (2 to 1.63%) and low grade (<1.63%) to understand the grade distributions of the nodules. Single-step transition frequencies and probabilities were calculated by moving progressively from grid point to next grid point for eight said directions¹ (figure 2). A FORTRAN IV program¹ and later modified² for ND 520 computer was used here.

Table 1 shows the transition frequencies calculated

for the 4 discrete states in 8 directions. The values are tabulated in a standard matrix form. The frequency values from one state to itself for all the eight directions show a consistency. The transition probabilities from one state to itself show a consistency for all the eight directions (table 2). For instance, the Markov transition probabilities, which are sensitive to direction, shows a consistency in all directions and reveal that the CIOB nodule grade distribution is weakly anisotropic. The transition frequencies and probabilities from one state to subsequent states demonstrate a high probability of encountering the same state when moving progressively in any of the studied directions. Even the probabilistic estimates give a fairly accurate grade predictions for any given point. The nodules in CIOB exhibit a definite progressive pattern of

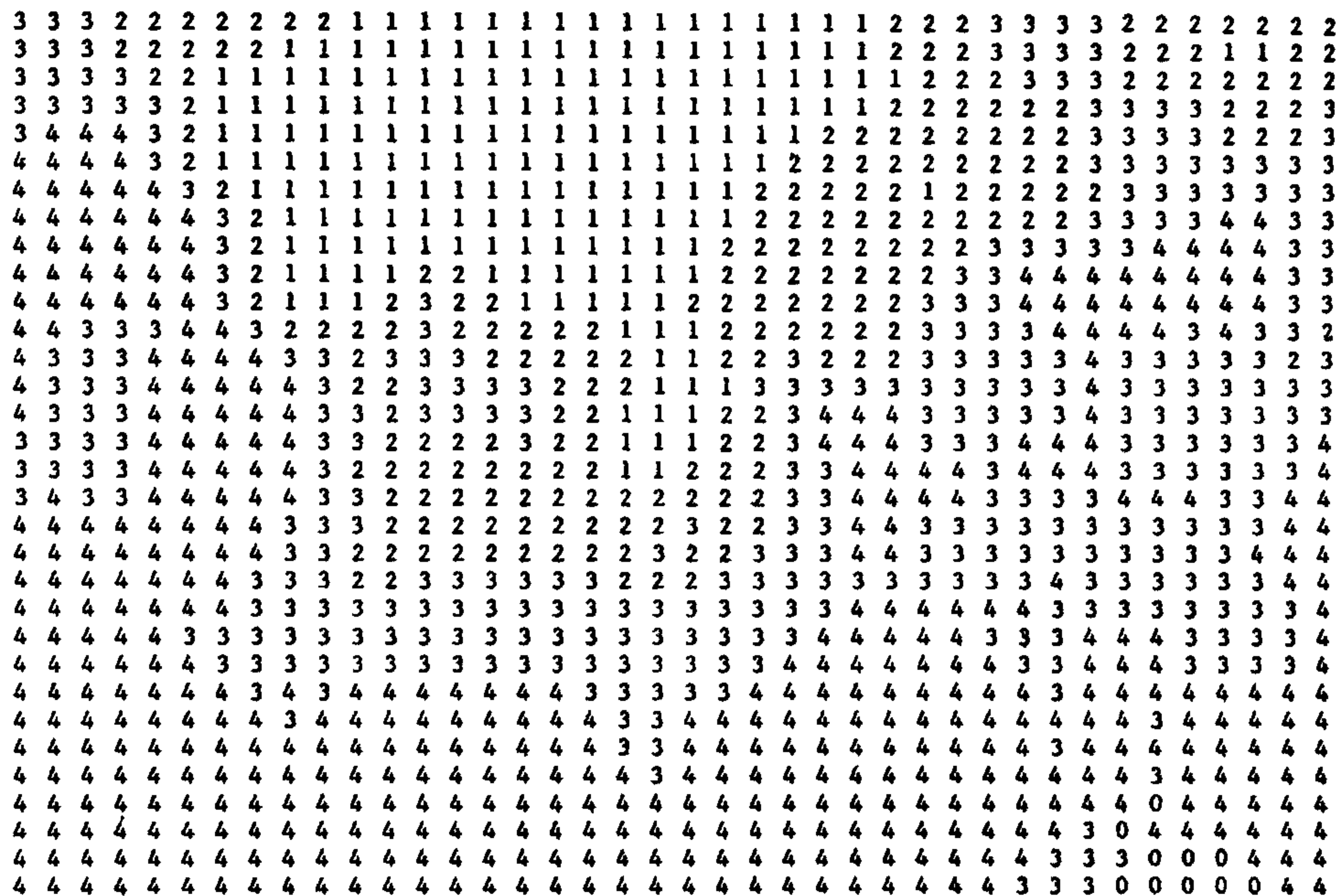


Figure 1. Digitized distribution pattern of grade (Ni + Cu + Co) in polymetallic nodules of CIOB representing four discrete states.

Table 2 Transition probabilities computed for eight directions shown in matrix tables

I	II	III	IV																																																																
<table border="1" style="width: 100%; border-collapse: collapse;"> <tr><td>0.89</td><td>0.11</td><td>0.01</td><td>0.00</td></tr> <tr><td>0.10</td><td>0.75</td><td>0.16</td><td>0.00</td></tr> <tr><td>0.00</td><td>0.11</td><td>0.74</td><td>0.15</td></tr> <tr><td>0.00</td><td>0.00</td><td>0.13</td><td>0.87</td></tr> </table>	0.89	0.11	0.01	0.00	0.10	0.75	0.16	0.00	0.00	0.11	0.74	0.15	0.00	0.00	0.13	0.87	<table border="1" style="width: 100%; border-collapse: collapse;"> <tr><td>0.89</td><td>0.11</td><td>0.00</td><td>0.00</td></tr> <tr><td>0.10</td><td>0.73</td><td>0.10</td><td>0.00</td></tr> <tr><td>0.00</td><td>0.10</td><td>0.73</td><td>0.10</td></tr> <tr><td>0.00</td><td>0.00</td><td>0.11</td><td>0.89</td></tr> </table>	0.89	0.11	0.00	0.00	0.10	0.73	0.10	0.00	0.00	0.10	0.73	0.10	0.00	0.00	0.11	0.89	<table border="1" style="width: 100%; border-collapse: collapse;"> <tr><td>0.86</td><td>0.14</td><td>0.00</td><td>0.00</td></tr> <tr><td>0.05</td><td>0.73</td><td>0.22</td><td>0.00</td></tr> <tr><td>0.00</td><td>0.05</td><td>0.75</td><td>0.21</td></tr> <tr><td>0.00</td><td>0.00</td><td>0.09</td><td>0.92</td></tr> </table>	0.86	0.14	0.00	0.00	0.05	0.73	0.22	0.00	0.00	0.05	0.75	0.21	0.00	0.00	0.09	0.92	<table border="1" style="width: 100%; border-collapse: collapse;"> <tr><td>0.94</td><td>0.06</td><td>0.00</td><td>0.00</td></tr> <tr><td>0.13</td><td>0.79</td><td>0.08</td><td>0.00</td></tr> <tr><td>0.00</td><td>0.14</td><td>0.75</td><td>0.11</td></tr> <tr><td>0.00</td><td>0.00</td><td>0.15</td><td>0.85</td></tr> </table>	0.94	0.06	0.00	0.00	0.13	0.79	0.08	0.00	0.00	0.14	0.75	0.11	0.00	0.00	0.15	0.85
0.89	0.11	0.01	0.00																																																																
0.10	0.75	0.16	0.00																																																																
0.00	0.11	0.74	0.15																																																																
0.00	0.00	0.13	0.87																																																																
0.89	0.11	0.00	0.00																																																																
0.10	0.73	0.10	0.00																																																																
0.00	0.10	0.73	0.10																																																																
0.00	0.00	0.11	0.89																																																																
0.86	0.14	0.00	0.00																																																																
0.05	0.73	0.22	0.00																																																																
0.00	0.05	0.75	0.21																																																																
0.00	0.00	0.09	0.92																																																																
0.94	0.06	0.00	0.00																																																																
0.13	0.79	0.08	0.00																																																																
0.00	0.14	0.75	0.11																																																																
0.00	0.00	0.15	0.85																																																																
V	VI	VII	VIII																																																																
<table border="1" style="width: 100%; border-collapse: collapse;"> <tr><td>0.86</td><td>0.12</td><td>0.00</td><td>0.00</td></tr> <tr><td>0.13</td><td>0.73</td><td>0.15</td><td>0.00</td></tr> <tr><td>0.01</td><td>0.19</td><td>0.67</td><td>0.14</td></tr> <tr><td>0.00</td><td>0.01</td><td>0.19</td><td>0.80</td></tr> </table>	0.86	0.12	0.00	0.00	0.13	0.73	0.15	0.00	0.01	0.19	0.67	0.14	0.00	0.01	0.19	0.80	<table border="1" style="width: 100%; border-collapse: collapse;"> <tr><td>0.83</td><td>0.15</td><td>0.02</td><td>0.00</td></tr> <tr><td>0.07</td><td>0.65</td><td>0.26</td><td>0.02</td></tr> <tr><td>0.00</td><td>0.08</td><td>0.66</td><td>0.26</td></tr> <tr><td>0.00</td><td>0.00</td><td>0.12</td><td>0.88</td></tr> </table>	0.83	0.15	0.02	0.00	0.07	0.65	0.26	0.02	0.00	0.08	0.66	0.26	0.00	0.00	0.12	0.88	<table border="1" style="width: 100%; border-collapse: collapse;"> <tr><td>0.82</td><td>0.10</td><td>0.01</td><td>0.00</td></tr> <tr><td>0.11</td><td>0.64</td><td>0.25</td><td>0.00</td></tr> <tr><td>0.00</td><td>0.07</td><td>0.66</td><td>0.27</td></tr> <tr><td>0.00</td><td>0.00</td><td>0.07</td><td>0.94</td></tr> </table>	0.82	0.10	0.01	0.00	0.11	0.64	0.25	0.00	0.00	0.07	0.66	0.27	0.00	0.00	0.07	0.94	<table border="1" style="width: 100%; border-collapse: collapse;"> <tr><td>0.89</td><td>0.12</td><td>0.00</td><td>0.00</td></tr> <tr><td>0.17</td><td>0.69</td><td>0.14</td><td>0.00</td></tr> <tr><td>0.00</td><td>0.16</td><td>0.65</td><td>0.19</td></tr> <tr><td>0.00</td><td>0.00</td><td>0.20</td><td>0.80</td></tr> </table>	0.89	0.12	0.00	0.00	0.17	0.69	0.14	0.00	0.00	0.16	0.65	0.19	0.00	0.00	0.20	0.80
0.86	0.12	0.00	0.00																																																																
0.13	0.73	0.15	0.00																																																																
0.01	0.19	0.67	0.14																																																																
0.00	0.01	0.19	0.80																																																																
0.83	0.15	0.02	0.00																																																																
0.07	0.65	0.26	0.02																																																																
0.00	0.08	0.66	0.26																																																																
0.00	0.00	0.12	0.88																																																																
0.82	0.10	0.01	0.00																																																																
0.11	0.64	0.25	0.00																																																																
0.00	0.07	0.66	0.27																																																																
0.00	0.00	0.07	0.94																																																																
0.89	0.12	0.00	0.00																																																																
0.17	0.69	0.14	0.00																																																																
0.00	0.16	0.65	0.19																																																																
0.00	0.00	0.20	0.80																																																																

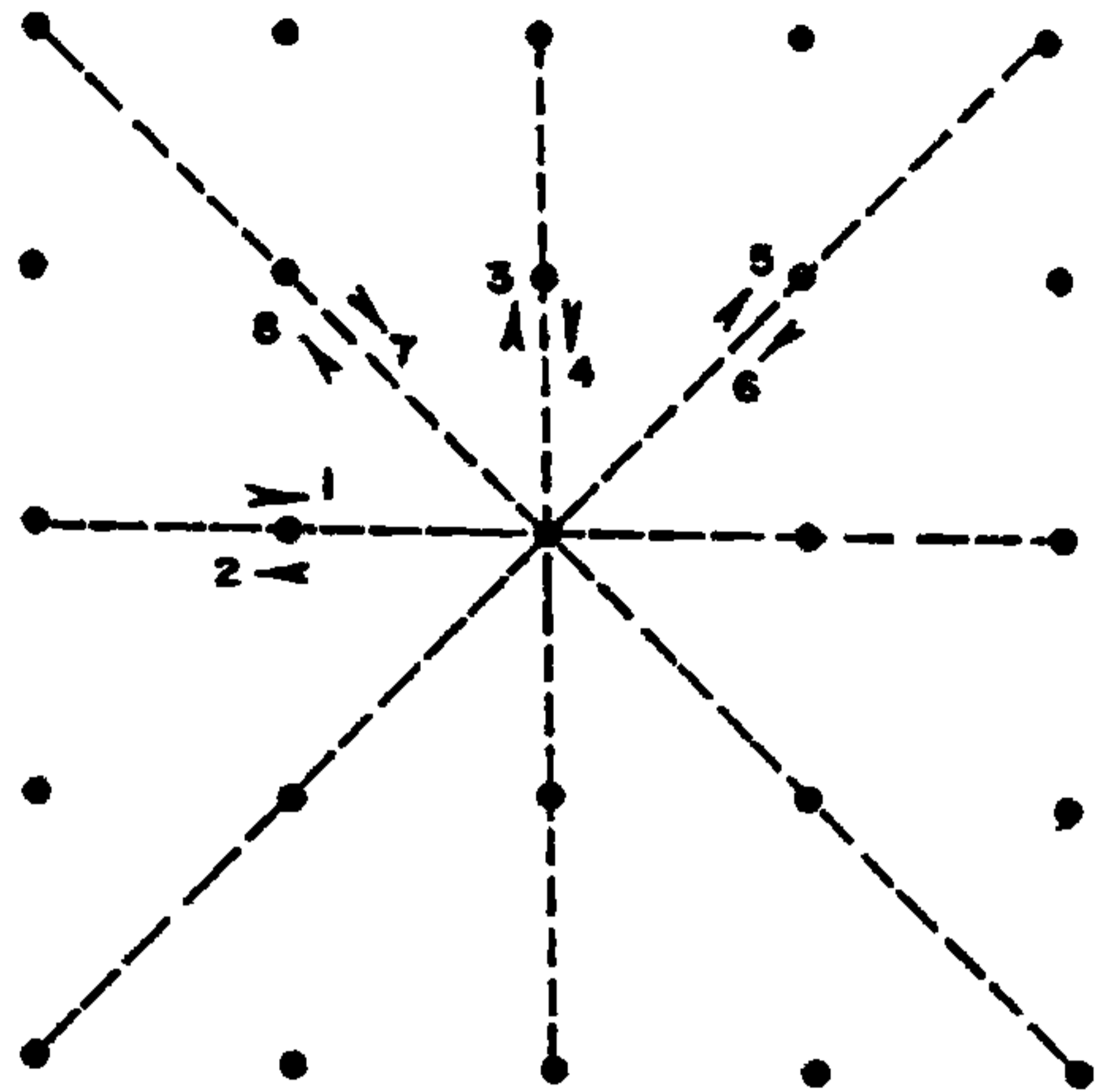


Figure 2. Diagram to illustrate eight directions for which transition probabilities are calculated (after Rohrllich *et al*¹).

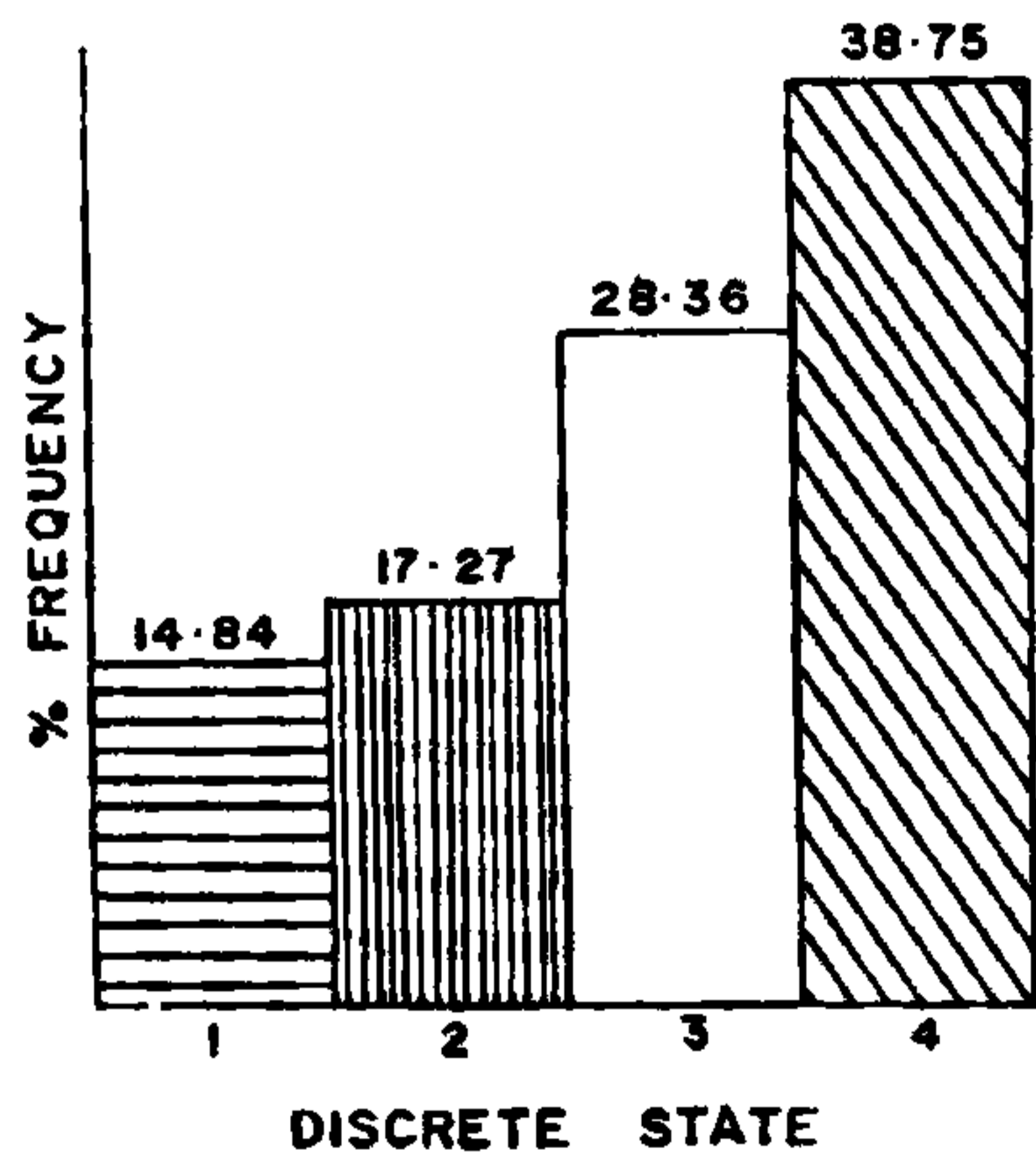


Figure 3. Frequency distribution of discrete states in CIOB nodule deposits. (1. Para-marginal > 2.47%; 2. Sub-marginal A 2.47-2%; 3. Sub-marginal B 2-1.63%; 4. Low grade < 1.63%).

grades. The grid distance between points is 25 km which may be taken as an optimum spacing while exploring these deposits. Obtaining more samples at a lesser (< 25 km) grid distance may prove little use as the deposit exhibits near isotropy. The values of grade, therefore, have a predictive value for the area falling between two successive grid points.

The chemical composition of nodules in CIOB

does not show a drastic variation within a few kilometers of distance (up to 25 km) and this supports the view expressed for Pacific Ocean nodules³. Considering 2% as the cut-off grade,

nearly 1/3 of the explored area in CIOB provides high grade regions (figure 3) for further evaluation and commercial mining.

The author thanks Dr G. P. Glasby for a critical review of this paper. The research was carried out with financial support from the DOD under their programme on Polymetallic Nodule Surveys.

5 August 1988

1. Rohrlich, V., Lin, C. and Harbaugh, J. W., *Comput. Geosci.*, 1985, 11, 2, 215.
2. Sudhakar, M., *NIO Technical Report No. NIO/TR/9/85*, 1985, p.26.
3. Cronan, D. S. and Tooms, J. S., *Deep-Sea Res.*, 1967, 14, 239.

ISOLATION OF STRAINS OF *ARTHROBACTER OXYDANS* INCAPABLE OF STEROID RING DEGRADATION

R. K. DUTTA, M. K. ROY and H. D. SINGH
*Biochemistry Division, Regional Research Laboratory,
Jorhat 785 006, India.*

FOR accumulation of pharmaceutically important 17-ketosteroids (17-KS) in sterol fermentation, the sterol side chain has to be cleaved selectively without degradation of the steroid nucleus. The critical reaction steps in the degradation of steroid nucleus are hydroxylation at the C-9 position and dehydrogenation at the C-1,2 position¹. When both reactions occur in the steroid nucleus, a very unstable compound, 9 α -hydroxy-1, 4-androstadien-3, 17-dione, is formed resulting in spontaneous cleavage of the B ring². Development of bacterial strains lacking in 9 α -hydroxylase and/or 1,2-dehydrogenase is therefore of interest.

The ability of *Arthrobacter oxydans* 317, a plasmid-bearing strain for complete degradation of β -sitosterol was reported previously³. In the presence of hydrophobic metal chelates which inhibit 9 α -hydroxylase, the strain produced 4-androstene-3, 17-dione (AD) and 1, 4-androstadien-3, 17-dione (ADD) from β -sitosterol but the production of these useful 17-KS was limited due to the lethal action of the inhibitors on the cells⁴. In this communication, the development of strains of *A. oxydans* 317 incapable

of degrading AD through treatment with sodium dodecyl sulphate (SDS), a potent plasmid curing agent⁵ and with 5-bromouracil (BU), a known mutagenic agent and the interesting behaviour of the new strains on the transformation of AD are reported.

A. oxydans 317 was grown in a number of shaken conical flasks containing 20 ml of nutrient broth (beef extract 5 g/l, peptone 5 g/l, NaCl 2.5 g/l) at 30°C. After 8 h of cultivation, SDS or BU solutions were added to separate flasks to give final concentrations of 0, 1, 4, 6, 8 and 10 mg/ml for SDS and 0, 20, 40, 60, 80 and 100 μ g/ml for BU and the cultivation was continued for another 8 h. One ml of the culture broth was plated on nutrient agar plates after suitable dilution, and viable cells were counted after incubation for 24 h at 30°C. Ability of the viable cells to degrade AD was adjudged by replica plating⁶ on mineral agar plates on which AD solution was spread. To study the transformation of AD, new strains refractory to AD were cultivated on a nutrient broth containing 0.5 g/l AD for 72 h at 30°C and the steroid metabolites were extracted with ethyl acetate and separated by preparative thin layer chromatography (PLC) using benzene/ethyl acetate (4:1) as the solvent phase⁷. The separated metabolites were identified from IR and NMR spectra and comparison with authentic samples.

Figure 1 shows that with increasing concentration of SDS in the treatment there was increasing appearance of strains incapable of utilizing AD until at 100 mg/ml of the chemical all the surviving cells were refractory to AD. With BU treatment a very small percentage (0.1) of the surviving cells were incapable of utilizing AD. From amongst the survivors incapable of utilizing AD, two strains (317 AI and 317 BI) from SDS treatment and four strains (ABUA1, BBUB2, ABUN1 and ABUN2) from BU treatment were isolated and transformations of AD by these strains were studied.

Strains 317AI and 317BI produced a single metabolite from AD as shown by a single metabolite spot in TLC having the same R_f value as the authentic testosterone. Its identity as testosterone was confirmed by spectral data [mp: 155°C; IR $\nu_{\text{max}}^{\text{KBr}}$ cm⁻¹: 3520 (17-OH), 1656, 1613 (Δ^4 -3-C=O); NMR (CDCl₃) δ : 0.8 (18-H), 1.8 (19 H), 3.66 (triplet, 17 OH), 5.73 (4 H)]. The results indicated the presence of active 17 β -hydroxylase in the strains. Inability to produce ADD from AD which is the normal pathway of metabolism possibly indicates that the strains lack 1,2-dehydrogenase. After incu-